Spectral line-by-line pulse shaping for optical arbitrary pulse-train generation

Zhi Jiang, Chen-Bin Huang, Daniel E. Leaird, and Andrew M. Weiner*

School of Electrical and Computer Engineering, Purdue University, 465 Northwestern Avenue, West Lafayette, Indiana 47907-2035, USA

**Corresponding author: amw@purdue.edu*

Received March 23, 2007; revised May 17, 2007; accepted May 19, 2007; posted May 24, 2007 (Doc. ID 81397); published August 3, 2007

We demonstrate optical arbitrary pulse-train generation using spectral line-by-line pulse shaping. The pulse train within each period can be independently controlled as specified.

OCIS codes: 320.5540, 320.7160.

1. INTRODUCTION

Pulse-shaping techniques, in which user-specified ultrashort pulse fields are synthesized via parallel manipulation of optical Fourier components, are now widely adopted [1]. Among the almost arbitrary waveforms enabled by pulse shaping, one subset with particular appeal involves generation and manipulation of optical pulse trains. Discrete pulse train packets (or bursts) have been generated by both Fourier transform pulse shapers [2–4] and direct space-to-time pulse shapers [5,6]. In these experiments the pulse train bursts were isolated in time and occupied a short time window compared to the laser repetition rate. Manipulation of continuous trains of pulses has attracted interest for many applications, including high-speed optical fiber communications, ultrafast optical signal processing, and photonically assisted generation of arbitrary millimeter-wave and microwave electromagnetic waveforms. Continuous pulse-train manipulation is usually implemented by all optical processing of pulses from high-repetition-rate (~10 GHz) mode-locked lasers [7–19]. The simplest example for continuous pulse-train operation is repetition rate multiplication (RRM) [7–15], which is usually implemented by spectral intensity or spectral phase filtering. In addition to simple RRM, continuous pulse trains with controllable patterns and envelopes have also been proposed and demonstrated [16–19]. In these demonstrations, high-repetition-rate mode-locked lasers (~10 GHz) are essential. In the frequency domain the output of such mode-locked lasers are characterized by an evenly spaced series of discrete spectral lines, with the frequency spacing equal to the pulse repetition rate. Recently we have demonstrated spectral line-by-line pulse shaping [20], in which we are able to resolve and manipulate individual spectral lines from mode-locked lasers at ~10 GHz. The capability of line-by-line pulse shaping immediately leads to efforts in pursuing optical arbitrary waveform generation [21]. In this paper we demonstrate optical arbitrary pulse-train generation (OAPTG) using spectral line-by-line pulse shaping, in which a pulse train spanning the entire period can be generated, and individual pulses can be independently manipulated to have different user-specified waveforms. This is in contrast to the pulse-train generation also using a Fourier transform pulse shaper but in the group of lines pulse-shaping regime [2–4], in which the pulse train spreads only to a very small fraction of the period. This limitation associated with the group of lines regime hinders capabilities for pulse-train generation significantly; for example, even two-times RRM is impossible.

2. PRINCIPLE AND TECHNIQUE OF LINE-BY-LINE SHAPING

For the purpose of OAPTG, the filter function has to be obtained first in order to properly control the spectral components of short periodic input pulses with our Fourier transforms line-by-line pulse shaper. Suppose the spectrum of the input pulses is $A(\omega)$; then $A(\omega)\exp(-i\omega\tau)$ corresponds to pulses with delay τ. Consider generating a simple pulse train with two identical unshaped pulses in each period; the spectrum is $A(\omega)+A(\omega)\exp(-i\omega\tau)$, and the resultant filter function is $H(\omega)=1+\exp(-i\omega\tau)$. This can be immediately generalized to a pulse train with many pulses in each period. Furthermore, individual pulses in each period can be shaped to desired waveforms in a different way. Mathematically, the filter function can be written as

$$H(\omega) = \sum_k a_k \exp(-i\omega\tau_k) H_k(\omega), \tag{1}$$

where the complex amplitude a_k allows us to control individual amplitudes and phases, the delay of the kth pulse in the period is determined by τ_k, and the waveform of the kth pulse is determined by its individual filter function $H_k(\omega)$. It is clear that all pulses are phase coherent. In our following experiments, the required spectral intensity and phase control are derived from the filter function in Eq. (1). The spectral intensity control is normalized to the maximum of $|H(\omega)|^2$. The number of pulses is limited by the period and pulse width. In most of our experiments,

the delays between pulses are sufficiently large, so pulses are well separated.

Line-by-line pulse shaping control for OAPTG is implemented by the well-developed ultrashort pulse-shaping techniques [1] using a fiber-coupled Fourier-transform pulse shaper that incorporates a 2×128 pixel liquid crystal modulator (LCM) array to independently control both the intensity and phase of each spectral line. In order to achieve line-by-line pulse shaping, great care is taken in the pulse-shaper design to improve resolution. A fiber-coupled pulse shaper with a reflective geometry is utilized as shown in Fig. 1, which includes a collimator/telescope combination to produce a collimated beam with ~18 mm diameter, a 1200 grooves/mm grating, a lens with 1000 mm focal length, an LCM with a 12.8 mm aperture and 2×128 independent pixels, a retroreflecting mirror, a circulator and a polarization controller (PC). The measured passband width is 2.6 GHz at the 3 dB points.

3. RESULTS AND DISCUSSION

Our experiments are performed using a harmonically mode-locked fiber laser producing 3.5 ps (FWHM) pulses centered near 1542 nm. The laser is running at 9.15 GHz, which precisely maps the spectral line spacing of the laser to the pixel spacing of the pulse shaper (we use two pixels to control one spectral line). The spectral lines from our mode-locked laser have sufficient stability (~5% frequency fluctuations of the individual spectral line positions with respect to the line spacing) for our demonstration. These short pulses are input into the line-by-line pulse shaper, which can be easily programmed to allow for convenient testing with various arbitrary optical pulse trains. The output of the pulse shaper is measured by an optical spectrum analyzer and intensity cross correlator using the initial unshaped pulse as the reference.

Figure 2 shows examples of repetition rate multiplication (RRM), which is a particular case of OAPTG. Figure 2A shows the input spectrum and pulses (intensity cross correlation). For phase-coherent pulses from a mode-locked laser, the phase difference between adjacent pulses is determined by the comb offset frequency or the absolute position of the spectral lines [22]. Without loss of generality, we assume that the phase difference between pulses is zero in our following discussion. Figure 2B and 2C show true RRM by periodically blocking one or multiple lines using spectral line-by-line intensity-only control [8–10]. This method results in both temporal intensity and phase RRM, so the phase difference between pulses remains zero after RRM. Here 2 times and 3 times RRM are demonstrated to generate pulse trains at 18.30 and 27.45 GHz repetition rate. This can be readily extended to higher RRM. Figure 2D shows another well-known approach for RRM—the temporal Talbot effect. The temporal Talbot effect is based on a spectral phase-only filter, which usually is implemented via a dispersive fiber or fiber Bragg grating [12–15]. In Fig. 2D we demonstrate two-fold RRM by applying spectral line-by-line phase control, where the spectral intensity remains essentially unchanged and spectral phases $[\pi/2\ 0\ \pi/2\ 0\ \ldots]$ are applied to individual lines. Note that the temporal Talbot effect leads to intensity-only RRM, and its temporal phase period remains the same as the input pulses. The temporal phase distribution in this example is $(\pi/4\ 3\pi/4\ \pi/4\ 3\pi/4\ \ldots)$ [12,13], according to the following discussion. RRM, by up to a factor of five based on the Talbot effect implemented using line-by-line pulse shaping, is reported in [23].

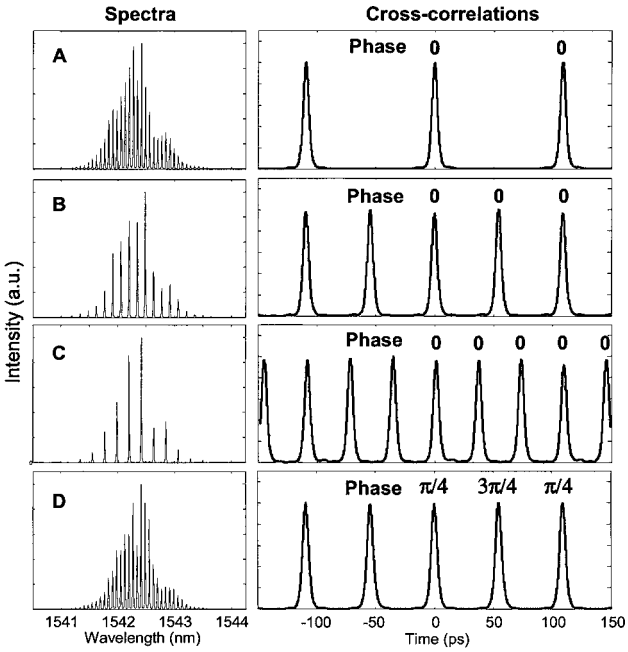

Fig. 2. OAPTG examples: repetition rate multiplication (RRM). A, input; B, C; 2 times and 3 times RRM by spectral-intensity-only control; D, 2 times RRM by spectral-phase-only control (temporal Talbot effect).

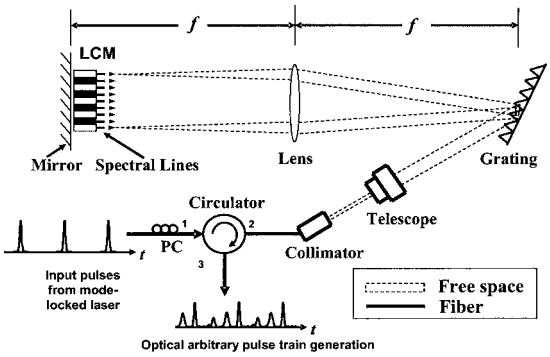

Fig. 1. Schematic diagram of the line-by-line pulse shaper.

It is easy to verify that these RRM approaches are particular cases of the proposed OAPTG. For example, for two-fold true RRM, the filter function is $H(\omega)=1+\exp(-i\omega T/2)$, where T is the input pulse train period. It exactly corresponds to a periodic spectral intensity-only filter (blocking every other spectral line) achieved by a line-by-line pulse shaper. Please note that here with a frequency comb we care only about the sampled filter function, with samples at frequency positions $2\pi m/T$ (m is an integer). For two-fold intensity RRM with the Talbot effect, the filter function is $H(\omega)=\exp(i\pi/4)+\exp(-i\omega T/2)\exp(i3\pi/4)$, which corresponds to a periodic spectral phase-only filter $[\pi/2\ 0\ \pi/2\ 0\ \ldots]$ applied by the line-by-line pulse shaper. After inverse Fourier transform it is clear that the resulting intensity-multiplied pulse

train has a temporal phase distribution of ($\pi/4$ $3\pi/4$ $\pi/4$ $3\pi/4$ ...). These examples demonstrate the capability for temporal intensity (here the intensities are made equal) and phase control on individual pulses in each period.

Figure 3A shows a pulse train with a binary pattern [1 1 0 1] in each period, where pulses are located at 0, $T/4$, and $3T/4$. Pulse intensities for 1 are very close to equal and are negligible for 0 (−25 dB lower). Both attributes still remain significant challenges in previous demonstrations [19]. To show arbitrary temporal intensity control rather than a binary pattern, an example of an intensity ladder pattern [0 1/4 1/2 1] is presented in Fig. 3B. Unlike simple RRM in Fig. 2 implemented by either a spectral intensity-only or a phase-only filter function, the patterns in Fig. 3 generally require simultaneous spectral intensity and phase control. (Note however that the pattern [1 1 0 1] can also be generated by a phase-only filter, e.g., with phases [0 0 2 arctan($\sqrt{2}$) 2 arctan($\sqrt{2}$) ...]). Also note that in Figs. 3A and 3B the pulses are evenly spaced, at the same temporal positions as in four-fold RRM, which results in periodic filter functions (periodic every four spectral lines). This is evident in the measured spectra. Figure 3C shows an example for arbitrary delay control in contrast to Figs. 3A and 3B. Three pulses in each period are located at 0, −25, and −75 ps, resulting in irregular pulse separations ($\Delta\tau_1$=50 ps, $\Delta\tau_2$=25 ps, $\Delta\tau_3$=34.3 ps). As a result, the filter function is not periodic any more, as clear from the spectrum in Figure 3C. These examples demonstrate the capability for arbitrary temporal intensity and delay control on individual pulses in each period.

In the above examples, all the pulses essentially keep the same profile as the input pulse. According to Eq. (1), pulses within a single period may also be controlled individually to have different user-specified waveforms. Figure 4A shows an example of three pulses in each period, with one pulse broadened. The temporal broadening is

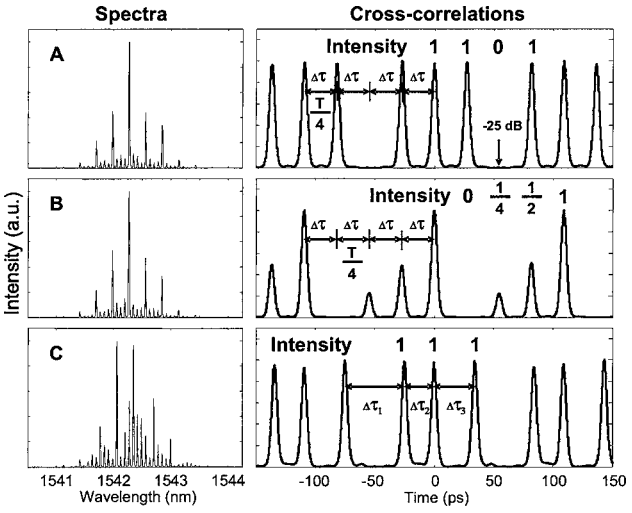

Fig. 3. OAPTG examples. A, binary pattern [1 1 1 0]; B, ladder pattern [0 1/4 1/2 1]; C, arbitrary delay ($\Delta\tau_1$=50 ps, $\Delta\tau_2$=25 ps, $\Delta\tau_3$=34.3 ps).

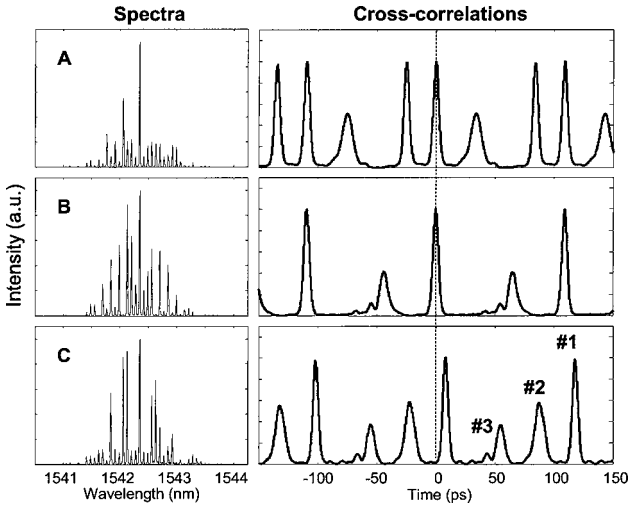

Fig. 4. OAPTG examples. A, one pulse width is broadened; B, one pulse has spectral cubic phase; C, pulse #1 has spectral linear phase, pulse #2 has spectral quadratic phase, pulse #3 has spectral cubic phase.

realized by applying an additional spectral quadratic phase on this pulse. Figure 4B shows an example of two pulses in each period, with an additional spectral cubic phase applied on one of the pulses. This pulse shows an oscillatory tail as expected, which is a sign of spectral cubic phase. Figure 4C shows an example with three pulses in each period, where pulse 1 has a linear spectral phase (corresponding to temporal delay), pulse 2 has a quadratic spectral phase (corresponding to temporal broadening), and pulse 3 has a cubic spectral phase (corresponding to an oscillatory temporal tail). These examples show the capability for OAPTG using line-by-line pulse shaping, in particular, the capability for achieving arbitrary waveform control on individual pulses in each period. Figure 5 shows the spectral line-by-line intensity and phase con-

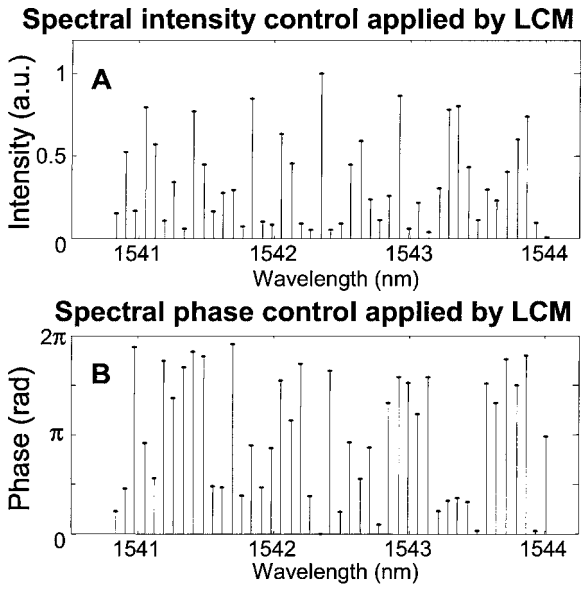

Fig. 5. Spectral line-by-line control applied by the LCM of pulse shaper for OAPTG pattern in Fig. 4C. A, spectral intensity control; B, spectral phase control.

trol applied by the LCM of the pulse shaper for the waveform pattern in Fig. 4C. At some locations the phase change per spectral line is π or more—a hallmark of operation in the line-by-line regime.

To generate a pulse train with well-separated individual pulses, the pulse width must be sufficiently short (actually in Fig. 4C, the pulse oscillatory tail with spectral cubic phase already starts overlapping with the adjacent pulse). Otherwise, pulses will overlap with each other, and the generated waveform is transformed from the regime of OAPTG to a more general regime—optical arbitrary waveform generation, where the waveform can spread throughout the entire period, which is another hallmark of line-by-line pulse shaping. In the current scalar OAPTG experiments where we are concerned with only one polarization, the intensity control in our pulse shaper is obtained through polarization control together with a polarizer at the output [1,3]. Therefore, we anticipate that vector OAPTG with the additional feature of polarization control can be readily achieved with minor modifications, similar to polarization pulse-shaping experiments that have been reported in the group of lines regime [24–27].

The super modes suppression in our laser is greater than 120 dBc/Hz by using a feedback control for cavity length stabilization. The comb offset frequency is not stabilized, so the spectral lines have a 5% frequency fluctuation (with respect to the line spacing). The spectral line fluctuation has almost no effect on the periodicity of the generated pulse train, since the periodicity is determined by the rf driving frequency on the actively mode-locked laser, which is quite stable. However, the spectral line fluctuation introduces distortion and/or noise on the generated pulse train and waveforms [20,28]. Although in our experiments the spectral lines show sufficient stability for the OAPTG demonstration, it is highly desirable to have laser sources with improved stability, since it has been realized that stabilized spectral lines play a critical role in the spectral line-by-line pulse shaping and optical arbitrary waveform generation [29].

4. CONCLUSION

We presented various examples of OAPTG using spectral line-by-line pulse shaping. We show that the filter functions required for OAPTG can be formulated in a straightforward analytical way. The generated pulse trains embody many particular cases, including RRM, the temporal Talbot effect, and pulse trains with specified pulse patterns and individual pulse shapes. Essentially, pulse trains with arbitrary waveform control exercised differently on the individual pulses within a single temporal period have been demonstrated.

ACKNOWLEDGMENTS

This work was supported by the Defense Advanced Research Projects Agency/Air Force Office of Scientific Research under grant FA9550-06-1-0189 and by the National Science Foundation under grant ECCS-0601692.

REFERENCES

1. A. M. Weiner, "Femtosecond pulse shaping using spatial light modulators," Rev. Sci. Instrum. **71**, 1929–1960 (2000).
2. A. M. Weiner and D. E. Leaird, "Generation of terahertz-rate trains of femtosecond pulses by phase-only filtering," Opt. Lett. **15**, 51–53 (1990).
3. M. M. Wefers and K. A. Nelson, "Generation of high-fidelity programmable ultrafast optical waveforms," Opt. Lett. **20**, 1047–1049 (1995).
4. C. W. Hillegas, J. X. Tull, D. Goswami, D. Strickland, and W. S. Warren, "Femtosecond laser pulse shaping by use of microsecond radio frequency pulses," Opt. Lett. **19**, 737–739 (1994).
5. D. E. Leaird and A. M. Weiner, "Femtosecond optical packet generation by a direct space-to-time pulse shaper," Opt. Lett. **24**, 853–855 (1999).
6. D. E. Leaird, S. Shen, A. M. Weiner, A. Sugita, S. Kamei, M. Ishii, and K. Okamoto, "Generation of high-repetition-rate WDM pulse trains from an arrayed-waveguide grating," IEEE Photonics Technol. Lett. **13**, 221–223 (2001).
7. D. S. Seo, D. E. Leaird, A. M. Weiner, S. Kamei, M. Ishii, A. Sugita, and K. Okamoto, "Continuous 500 GHz pulse train generation by repetition-rate multiplication using arrayed waveguide grating," Electron. Lett. **39**, 1138–1140 (2003).
8. T. Sizer II, "Increase in laser repetition rate by spectral selection," IEEE J. Quantum Electron. **25**, 97–103 (1989).
9. P. Petropoulos, M. Ibsen, M. N. Zervas, and D. J. Richardson, "Generation of a 40-GHz pulse stream by pulse multiplication with a sampled fiber Bragg grating," Opt. Lett. **25**, 521–523 (2000).
10. K. Yiannopoulos, K. Vyrsokinos, E. Kehayas, N. Pleros, K. Vlachos, H. Avramopoulos, and G. Guekos, "Rate multiplication by double-passing Fabry–Pérot filtering," IEEE Photonics Technol. Lett. **15**, 1294–1296 (2003).
11. C.-B. Huang and Y. C. Lai, "Loss-less pulse intensity repetition-rate multiplication using optical all-pass filtering," IEEE Photonics Technol. Lett. **12**, 167–169 (2000).
12. J. Azana and M. A. Muriel, "Temporal self-imaging effects: theory and application for multiplying pulse repetition rates," IEEE J. Sel. Top. Quantum Electron. **7**, 728–744 (2001).
13. S. Longhi, M. Marano, P. Laporta, and V. Pruneri, "Multiplication and reshaping of high-repetition-rate optical pulse trains using highly dispersive fiber Bragg gratings," IEEE Photonics Technol. Lett. **12**, 1498–1500 (2000).
14. D. Pudo and L. R. Chen, "Tunable passive all-optical pulse repetition rate multiplier using fiber Bragg gratings," J. Lightwave Technol. **23**, 1729–1733 (2005).
15. S. Atkins and B. Fischer, "All-optical pulse rate multiplication using fractional Talbot effect and field-to-intensity conversion with cross-gain modulation," IEEE Photonics Technol. Lett. **15**, 132–134 (2003).
16. J. D. McKinney, D. S. Seo, D. E. Leaird, and A. M. Weiner, "Photonically assisted generation of arbitrary millimeter-wave and microwave electromagnetic waveforms via direct space-to-time optical pulse shaping," J. Lightwave Technol. **21**, 3020–3028 (2003).
17. B. Xia and L. R. Chen, "A direct temporal domain approach for pulse-repetition rate multiplication with arbitrary envelope shaping," IEEE J. Sel. Top. Quantum Electron. **11**, 165–172 (2005).
18. B. Xia and L. R. Chen, "Ring resonator arrays for pulse repetition rate multiplication and shaping," IEEE Photonics Technol. Lett. **18**, 1999–2001 (2006).
19. B. Xia, L. R. Chen, P. Dumais, and C. L. Callender, "Ultrafast pulse train generation with binary code patterns using planar lightwave circuits," Electron. Lett. **42**, 1119–1120 (2006).
20. Z. Jiang, D. S. Seo, D. E. Leaird, and A. M. Weiner, "Spectral line-by-line pulse shaping," Opt. Lett. **30**, 1557–1559 (2005).
21. Z. Jiang, D. E. Leaird, and A. M. Weiner, "Line-by-line

pulse shaping control for optical arbitrary waveform generation," Opt. Express **13**, 10431–10439 (2005).
22. S. T. Cundiff, 'Phase stabilization of ultrashort optical pulses," J. Phys. D **35**, R43–R59 (2002).
23. J. Caraquitena, Z. Jiang, D. E. Leaird, and A. M. Weiner, "Tunable pulse repetition-rate multiplication using phase-only line-by-line pulse shaping," Opt. Lett. **32**, 716–718 (2007).
24. T. Brixner and G. Gerber, "Femtosecond polarization pulse shaping," Opt. Lett. **26**, 557–559 (2001).
25. M. Akbulut, R. Nelson, A. M. Weiner, P. Cronin, and P. J. Miller, "Broadband polarization correction with programmable liquid-crystal modulator arrays," Opt. Lett. **29**, 1129–1131 (2004).
26. M. Akbulut, A. M. Weiner, and P. J. Miller, "Wideband all-order polarization mode dispersion compensation via pulse shaping," Opt. Lett. **30**, 2691–2693 (2005).
27. L. Polachek, D. Oron, and Y. Silberberg, "Full control of the spectral polarization of ultrashort pulses," Opt. Lett. **31**, 631–633 (2006).
28. C.-B. Huang, Z. Jiang, D. E. Leaird, and A. M. Weiner, "The impact of optical comb stability on waveforms generated via spectral line-by-line pulse shaping," Opt. Express **14**, 13164–13176 (2006).
29. Z. Jiang, D. E. Leaird, and A. M. Weiner, "Optical processing based on spectral line-by-line pulse shaping on a phase modulated CW laser," IEEE J. Quantum Electron. **42**, 657–665 (2006).